MECHANISTIC OUTCOMES OF LIPID CORE ON SOLID LIPID NANOPARTICLE CHARACTERIZATION

Juna B. Chacko[a,b]*, Gudanagaram R. Vijayasankar[a], Bendi S. Venkateswarlu[a] and Margret C. Rajappa[a]

(Received 30 January 2023) (Accepted 20 January 2024)

ABSTRACT

In our present study, solid lipid nanoparticles were fabricated by modified double emulsification followed by ultracentrifugation method. The SLNs of the anti-HIV drugs lamivudine, tenofovir disoproxil fumarate and efavirenz were synthesized using lipids Compritol 888 ATO, glyceryl monostearate, stearic acid and emulsifiers soy lecithin and Pluronic®F68. The synthesized SLNs were characterized for compatibility studies, mean particle size, PDI, zeta potential, surface morphology and entrapment studies. The higher amount of Compritol based SLNs formulation showed maximum entrapment efficiency with comparatively larger sized, homogenous particles. All the lipid based SLNs possessed no incompatibilities and showed high stability profiles. Based on the results of surface morphology, zeta potential and high entrapment efficiency values, the optimum lipid for SLNs formulation among the other lipids was determined to be Compritol 888 ATO.

Keywords: Solid lipid nanoparticle, Compritol 888 ATO, glyceryl monostearate, stearic acid, entrapment efficiency

INTRODUCTION

Solid lipid nanoparticles (SLNs) are generally regarded as a safe (GRAS) novel drug delivery system for hydrophilic and hydrophobic drugs for parenteral, oral, nasal or pulmonary routes[1]. Ideal SLNs are expected to enhance the drug entrapment, drug targeting, bioavailability and sustained action of drug, improve the pharmacokinetic behaviour and reduces the constraints such as drug leakage, burst release and low efficacy profile associated with conventional drug delivery system. SLNs can be considered as a value-added carrier by the proper selection of biodegradable lipids, surfactants and biocompatibility in human beings. SLNs are a new generation lipid system which is made up of solid lipid triglycerides, waxes, fatty acids, steroids, emulsifiers and water as solvent[2]. The combination of emulsifiers efficiently prevents the particle agglomeration and its proper selection depends on the choice of administration routes. The solid lipid of physiological nature drastically reduces the toxicity behaviour, reduces the mobility of incorporated drugs and also coalescence and accretion of particles, which attains an exclusive goal of stability and prolonged drug release[3,4].

Solid lipid nanoparticles were developed by several methods which are represented in various reviews as mentioned below;

- High shear homogenization (hot homogenization and cold homogenization)
- Solvent emulsification evaporation method
- Multiple emulsification solvent evaporation method
- Membrane contractor method

High shear homogenization is the most reliable and effective method as it offers SLNs with narrow size distribution, high drug loading, avoidance of organic solvent, better interaction of phases at the interphases and improved acceptability of homogenization equipment for the researchers. Nowadays, many biomedical and pharmaceutical innovators are focussed on the modification of high-pressure homogenization and ultrasonication methods, as it embraces great promise for achieving the goals by obtaining reduced particle size with maximum loading[5,6,7].

SLNs have been explored through various application routes, including oral, parenteral (subcutaneous, intravenous, intramuscular), pulmonary, rectal, ophthalmic and topical (in dermatological treatment). The

[a] Department of Pharmaceutics, Vinayaka Mission's Research Foundation (Deemed to be University), NH47, Sankari Main Road, Salem – 636 308, Tamil Nadu, India

[b] Department of Pharmaceutics, Caritas College of Pharmacy, Caritas educity, Ettumanoor, Kottayam – 686 631, Kerala, India

* For Correspondence: E-mail: junachacko25@gmail.com

https://doi.org/10.53879/id.61.02.13881

Table I: SLNs formulation compositions

Ingredient	F1	F2	F3	F4	F5	F6
Compritol 888ATO (mg)	100 mg	--	--	200 mg	---	----
Glyceryl monostearate (mg)	-	100 mg	---	---	200 mg	---
Stearic acid (mg)	-	--	100 mg	---	---	200 mg
Soy lecithin	25 mg	25 mg	25 mg	25 mg	25 mg	25 mg
TDF, LM, EFZ	5 mg each	5 mg each	5 mg each	5 mg each	5 mg each	5 mg each
Primary organic to external aqueous phase ratio	1:2	1:2	1:2	1:2	1:2	1:2

administration route and distribution process determine the *in vivo* fate of SLNs, probably degradation by splitting of ester linkage by lipases. The acceptable dosage forms of SLNs through oral routes may include tablets, capsules, pellets and aqueous dispersions[8]. The effect of micro environment pH of stomach and presence of food will likely have a significant impact on SLNs performance, although to our knowledge, no experimental data have been published on this topic. SLNs are ideal for parenteral administration because they possess good stability, extensive circulation time in the microvascular system, and negligible agglomeration after lyophilization. Pulmonary SLNs delivery suggested high selectivity for targeting with low systemic circulation. The incorporation of SLNs dispersion with low lipid content upto 5 % into ointments and gels make it acceptable for transdermal administration. Regardless of the routes of administration, SLNs have several potential applications, including CNS diseases, tumor targeting, gene vector carrying, lymphatic targeting, neurological diseases, AIDS, psychiatric disorders and for antitubercular chemotherapy[9,4,10,11].

In our research, we are focussing on the w/o/w double emulsification method for the internalization of hydrophilic drugs in the internal aqueous phase, which exert a hindrance for the leakage of drugs into external aqueous phase during formulation. Meanwhile, the lipophilic drugs are entrapped in the internal lipid matrix by using a combination of emulsifying agent and stabilizers. Thus, SLNs open up a new vista for multiple drugs delivery.

MATERIALS AND METHODS

Materials

Tenofovir disoproxil fumarate (TDF), lamivudine (LM) and efavirenz (EFZ) were obtained from Cipla, India. Compritol 888 ATO (glyceryl behenate) was obtained from Gattefosse, Mumbai, India. Glyceryl monostearate, stearic acid, Pluronic F® 68, and soy lecithin, were procured from Sigma Aldrich, India. HPLC grade distilled water was used for preparation.

Preparation of lamivudine, tenofovir disoproxil fumarate, efavirenz-loaded solid lipid nanoparticle (LM-TDF-EFZ-SLNs)

Modified double emulsification and solvent evaporation methods were used to synthesize the solid lipid nanoparticles[12-15]. The internal aqueous phase was created by dissolving the hydrophilic drugs TDF and LM in 2 mL of distilled water. The organic phase was comprised of the lipid i.e Compritol 888ATO/ glyceryl monostearate/ stearic acid and the hydrophobic drug EFZ and soy lecithin, were dissolved in 10 mL acetone: methanol (2:1 ratio). The aqueous phase was poured (500 µL min^{-1}) into the organic phase with continuous homogenization at 25000 rpm for 10 minutes. The primary w/o emulsion formed was then introduced into the continuous phase containing distilled water, an electrolyte NaCl (100mM), Pluronic® F68 with continuous homogenization for 10 minutes at 25000 rpm (Heidolph homogeniser silent crusher). The coarse w/o/w emulsion formed was sonicated (45 % amplitude and 20/10 pulse regime on/off cycle) for 2 minutes to get fine emulsion and kept overnight on a magnetic stirrer for solvent evaporation. The resulting w/o/w emulsion was centrifuged at 13,000 rpm at 4 ^{0}C for 4 h. The sedimented nanoparticles were washed thrice using deionized water and lyophilized[16]. The composition of SLNs is depicted in Table I.

Compatibility studies

The FTIR spectra of TDF, LM, EFZ, pure drugs physical mixture (1:1:1), Poloxomer 188, Compritol

888ATO, stearic acid, glyceryl monostearate and drugs loaded SLNs were recorded.

Entrapment efficiency

The percentage entrapment efficiency (EE %) of TDF, LM and EFZ were estimated by indirect ultracentrifugation method[17,18]. About 10 mL of SLNs dispersion was centrifuged for 4 h at 13,000 rpm at 4 °C. The concentration of unentrapped drugs within the supernatant were analyzed spectrophotometrically at 247 nm, 259 nm and 272 nm and individual drug concentration were calculated by simultaneous equation method[19-22].

$$C_{EFZ} = A_1(ay_2az_3 - az_2ay_3) - ay_1(A_2az_3 - az_2A_3) + \frac{az_1(A_2ay_3 - ay_2A_3)}{ax_1(ay_2az_3 - az_2ay_3)}$$
$$- ay_1(ax_2az_3 - az_2ax_3) + az_1(ax_2ay_3 - ay_2ax_3)$$

$$C_{TDF} = ax_1(A_2az_3 - az_2A_3) - A_1(ax_2az_3 - az_2ax_3) + \frac{az_1(ax_2A_3 - A_2ax_3)}{ax_1(ay_2az_3 - az_2ay_3)}$$
$$- ay_1(ax_2az_3 - az_2ax_3) + az_1(ax_2ay_3 - ay_2ax_3)$$

$$C_{LM} = ax_1(ay_2A_3 - A_2ay_3) - ay_1(ax_2A_3 - A_2ax_3) + \frac{A_1(ax_2ay_3 - ay_2ax_3)}{ax_1(ay_2az_3 - az_2ay_3)}$$
$$- ay_1(ax_2az_3 - az_2ax_3) + az_1(ax_2ay_3 - ay_2ax_3)$$

where

A_1, A_2, A_3-Absorbance of sample at 247nm, 259 nm, 272 nm

ax_1, ax_2, ax_3- Absorptivity of efavirenz at 247 nm, 259 nm, 272 nm

ay_1, ay_2, ay_3- Absorptivity of tenofovir disoproxil fumarate at 247 nm, 259 nm, 272 nm

az_1, az_2, az_3- Absorptivity of lamivudine at 247 nm, 259 nm, 272 nm

The % EE was calculated as follows:

$$\% EE = \frac{(Total\ amount\ of\ drug\ taken - Unentrapped\ drug) \times 100}{Total\ amount\ of\ drug\ taken}$$

Particle size, PDI, zeta potential

Photon correlation spectroscopy (Nano ZS90 Malvern zeta sizer) was used to quantify the particle size distribution, polydispersity index and zeta potential of SLNs at a fixed angle of 90^0 at 25 °C.

Surface morphology

The shape and surface morphology of SLNs were investigated by scanning electron microscopy (JEOL JSM-6390) scanning electron microscope). The solid lipid nanoparticles were fixed on adequate support and coated with platinum using platinum sputter module (JFC-1100, JEOL Ltd), in a high vacuum evaporator for 5 minutes at 20 mA.

RESULTS

FT-IR Studies

The FTIR spectrum of TDF exhibited peaks at 2983.27 cm^{-1} and 1094.84cm^{-1}, corresponding to CH aliphatic stretching, and C-O group stretching, respectively[27]. FTIR peaks at 1673.55 and 1751.27 cm^{-1} represented C=O stretching from fumarate portion of TDF, while the peaks at 3218.21 cm^{-1} and 1621.91 cm^{-1} corresponded to NH_2 stretching vibration and N-H bending. The peak at 696.60 cm^{-1} and 723.96 cm^{-1} suggested the presence of aromatic ring without plane bending and out of plane CH_2 bending. IR absorption band at 1183.97 cm^{-1} confirms P=O stretching.

The IR absorption peaks of lamivudine at 1285.18 and 1158.33 cm^{-1} is due to symmetrical and asymmetrical stretching of the oxathiolane ring's C-O-C system. The band at 1632.96 cm^{-1} is due to C=O–NR2 stretching, which overlaps the band due to N–H bending at 1607.07 cm^{-1}.The broad band peaks at 3322.5 and 3193.91 cm^{-1}, confirm the presence of amino and hydroxyl groups of the drug[23,24].

The characteristic peaks in the FTIR spectrum of efavirenz (EFZ) are strong N-H stretch at 3311.96 cm^{-1}, CH stretch at 2248.55 cm^{-1}, C=O stretch at 1741.88 cm^{-1}, C-F stretch at 1428.56, 1395.99 cm^{-1} and C-Cl stretch[25,26] at 1037.64 cm^{-1}.

In the FTIR spectrum of 1:1:1 physical mixture of tenofovir disoproxil fumarate: lamivudine: efavirenz, all the characteristics peaks are present but the major sharp peaks in the pure drug spectrum are changed to broad bands due to the overlapping of spectra, which indicate that there were no chemical interactions between the drugs.

The FTIR spectra of Compritol 888 ATO depicted typical bands at 3308.34 cm^{-1}, at 2847.75 cm^{1} and at 1733.38 cm^{-1} due to -OH stretch, -CH stretch and -C=O stretch. The presence of methylene groups was confirmed by many vibrational bands in the range of 700 and 1500 cm^{-1} [27].

In the FTIR spectra of Pluronic®F68, the major peak for % transmittance is observed at 2879.50 cm^{-1} which corresponded to the stretching vibration of C–H group and another peak at 3460.09 cm^{-1}, which was assigned to the -OH group[28].

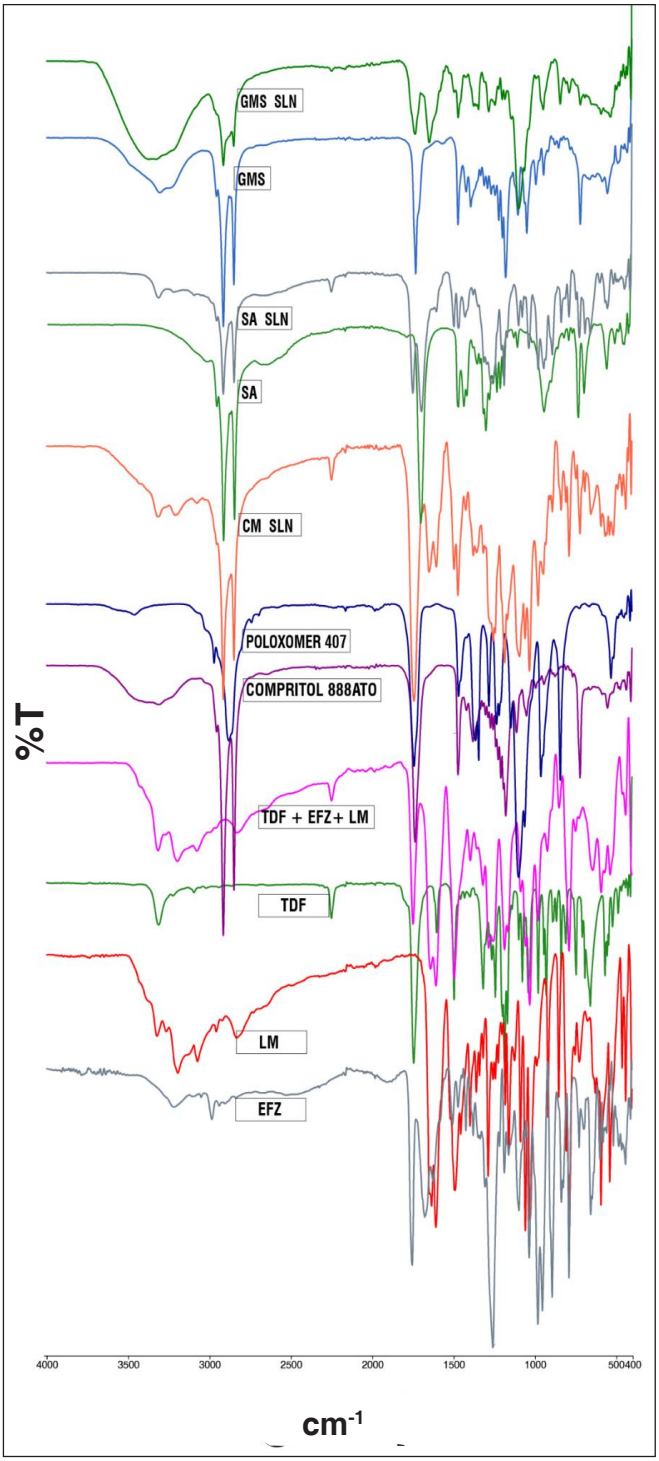

Fig. 1: FTIR spectrum (from bottom to top) efavirenz; lamivudine; tenofovir disoproxil fumarate; physical mixture (1:1:1); Compritol 888 ATO; Pluronic®F 68; compritol SLNs, stearic acid; stearic acid SLNs; glyceryl monostearate; glyceryl monostearate SLNs

In the spectra of TDF, LM, EFZ loaded compritol 888 ATO lipid based SLNs, all the major peaks due to the functional groups such as -OH, -NH, C-F, C=O, C-H, C-Cl, C-F were not changed, so it may be concluded that there was no interaction between the drugs and excipients. However, there might be some fluctuation in peak intensities since several functional groups with a given band width overlap.

The FTIR spectra of GMS showed characteristic bands of -OH stretch at 3304.04cm^{-1}, C-H stretch at 2913.55 cm^{-1} and due to ester carbonyl functional group stretch at 1729.83 cm^{-1}.

The band in the region between 3500-3000 cm^{-1} became more pronounced and this may be caused by the spectral overlapping of stretching vibrations of -OH and -NH functional groups present in drugs and GMS. There was no chemical reaction between the drugs and the lipid core, as evidenced by the lack of new bands in TDF, LM, and EFZ-SLNs; instead, the drugs were only dissolved or dispersed in the lipid core of GMS[29].

In the spectrum of stearic acid, there were adsorption peaks at 2913.94 cm^{-1} and 2846.93 cm^{-1}, attributed to the aliphatic –CH– chain asymmetric and symmetric stretching vibrations, respectively. The peaks at 1694.14 cm^{-1} and 1464.41 cm^{-1} were assigned to the characteristic stretching and bending vibration of the CO group of carboxylic acid.

In TDF, LM, EFZ loaded stearic acid based SLNs a broad band in the region of 3500-3000 cm^{-1} represented the merging of peaks due to -OH and -NH stretching vibrations. All the characteristic peaks present in the individual spectra of drugs as well as stearic acid were not changed, representing the compatibility between the drugs and excipients.

Table II: Entrapment efficiency of SLNs formulations

Formulation	Lamivudine EE %	TDF EE %	Efavirenz EE %
F1	55.01±0.26	55.37±0.05	60.21±0.73
F2	47.36±0.15	47.27±0.23	52.61±0.31
F3	46.31±0.47	47.04±0.07	50.14±0.17
F4	63.8±0.28	64.52±0.42	68.4±0.37
F5	53.35±0.61	51.37±0.54	60.64±0.71
F6	54.28±0.37	52.81±0.51	61.31±0.43

Entrapment efficiency

Table II summarizes the data of % entrapment efficiency for all formulations and shows that the amount lipid core can affect the EE of drugs. From the data, it was clear that the entrapment efficiency of loaded targets was identical across all formulations, including an equal amount of lipid, (within ± 2 % variation in loaded drugs) whether in the form of free fatty acid or glycerides. But the formulations containing triglycerides with high chain length (Compritol 888 ATO) demonstrated about 8 % greater drug entrapment than stearic acid and glyceryl monostearate SLNs.

Particle size, PDI, zeta potential

The average particle sizes of all SLNs formulations with 100 mg lipid possessed a mean size ranging from 143 nm to 212 nm and with 200 mg lipid the size ranged from 181nm to 337 nm (Fig. 2)[30]. The PDI values of SLNs should be less than 0.4, indicating the monodispersity of formulations.

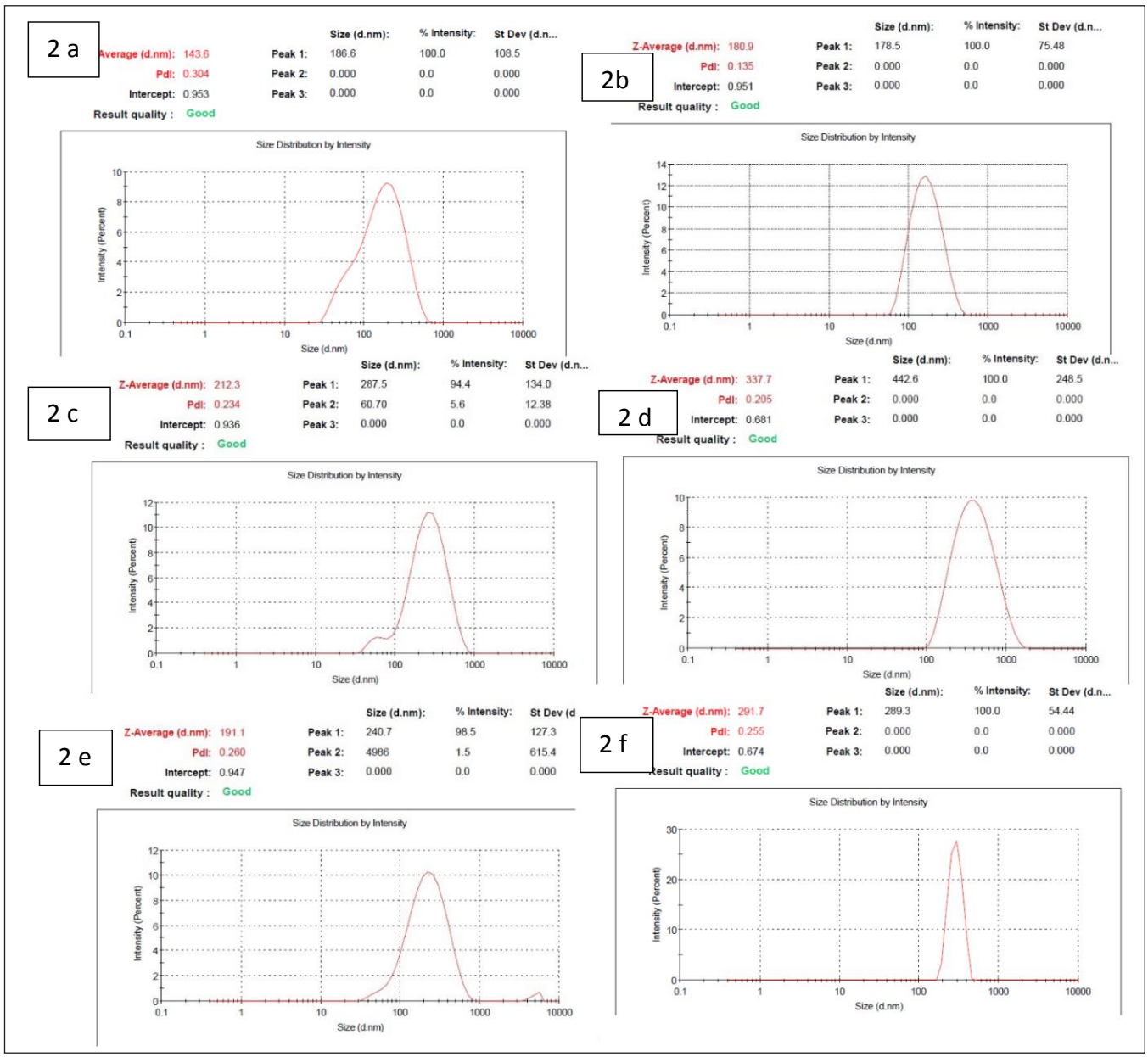

Fig. 2: Average particle size; stearic acid SLNs (100 mg) [2 a]; stearic acid SLNs (200 mg) [2 b]; Compritol SLNs (100 mg) [2c]; Compritol SLNs (200 mg) [2d]; Glyceryl monostearate SLNs (100 mg) [2e]; Glyceryl monostearate SLNs (200 mg) [2f]

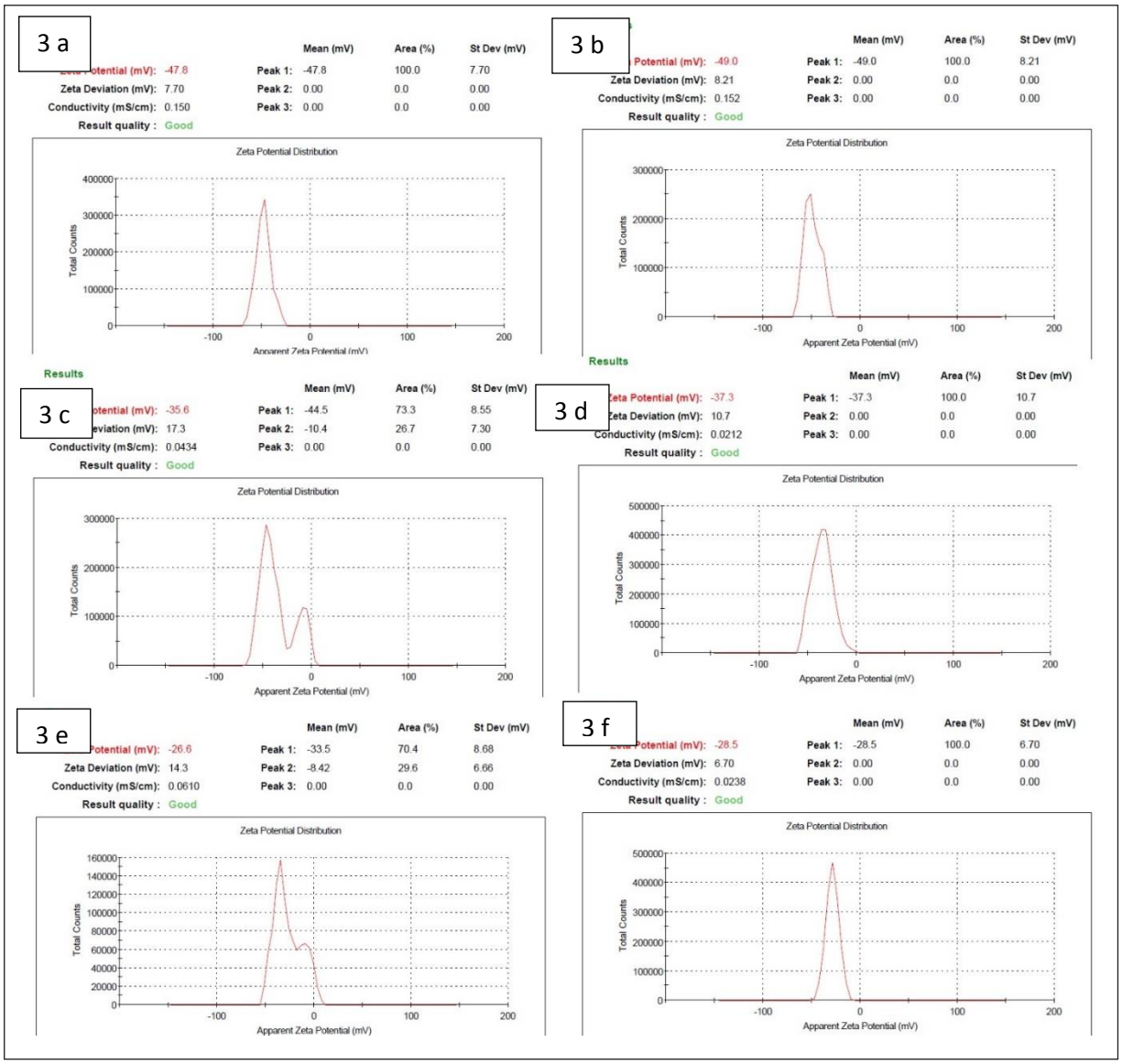

Fig. 3: Zeta potential values; Stearic acid SLNs (100 mg) [3 a]; Stearic acid SLNs (200 mg) [3 b]; Glyceryl monostearate SLNs (100 mg) [3c]; Glyceryl monostearate SLNs (200 mg) [3d]. Compritol SLNs (100 mg) [3e]; Compritol SLNs (200 mg) [3f]

All formulations exhibited a negative zeta potential with highest value of -49.0 for SA- SLNs and was lowest with CM-SLNs[31,32]. An overview of zeta potential values is reported in Fig. 3.

Shape and surface morphology

Fig. 4 shows the formulation of F4 with higher Compritol content. The morphology of particles appears to be uniform, smooth and spherical in shape. Lyophilization did not cause aggregation and the particles exist as uniform sized, separate entities. Shape plays an important role in drug delivery. A spherical particle flowing through a vessel exhibits streamline motion if it is not under the influence of an external force.

DISCUSSION

The FTIR spectra of physical mixture of drugs, lipids and formulation in Fig. 1 indicated no major loss or shifting of functional peaks, hence it was confirmed that there was no interaction between drugs and lipids.

The higher concentration of lipids provides enough space for target lodging with minimal drug escape to external phase and achieves maximum drug entrapment.

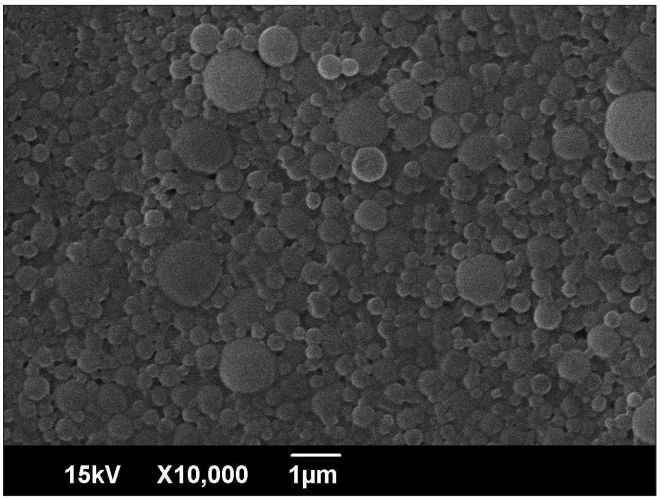

Fig. 4: SEM image F4 formulation of Compritol SLNs (more homogenous particles relating to SA SLNs & GMS SLNs)

The long chain fatty acids in Compritol offered the interbedding of targets in the solid matrix and inter molecular drug enrichment may ascribe the highest entrapment efficiency of F4> F1> F6> F5> F3> F2[33].

From the results of mean particle size and PDI, an increase in lipid content increases the particle size but not in a linear pattern; not much significant effect on PDI values. The increase in particle size may be due to insufficient surfactant for emulsification, resulting in greater particle agglomeration. As revealed in Fig. 2, the greatest particle sizes were shown by Compritol 888 ATO, followed by glyceryl monostearate and stearic acid SLNs. Size variations could be explained by variations in the chain lengths and melting point of the lipids utilized. A solid lipid, Compritol 888 ATO, with a melting point of 69.0–74.0 °C, is built on glycerol esters of behenic acid (C22), with behenic acid accounting for more than 85% of the fatty acid content. Other fatty acids (C16–C20) are also present. Glyceryl monostearate (C21) (m.p 50–55 °C) and stearic acid (C18) (m.p. 70 °C) were also investigated. In comparison to glyceryl monostearate and stearic acid SLNs, Compritol 888 ATO may have bigger particle size due to its high melt temperature, and its long hydrocarbon chain length, which in turn increases its viscosity[34].

The highest zeta potential attributed to SA-SLNs might be due to surface coverage of SLN with negatively charged stearin. Furthermore, when the nature of lipid core is changed to glycerides and glyceryl behenate moieties, a continuous decrease in negative value of zeta potential is observed. Moreover, a slight increase in zeta potential value was observed with increasing lipid concentration, but no linear correlation was proved.

CONCLUSION

Based on the outcomes, it can be concluded that all the lipids are suitable for the entrapment of tenofovir disoproxil fumarate, lamivudine and efavirenz. Furthermore, SLNs developed from the lipid core Compritol 888 ATO is optimal for further *in vivo* studies as it had high drug loading and better zeta potential values with homogenous, discrete particles.

REFERENCES

1. Chacko J. B. and Sankar G.R.V.: Lymphatic targeted drug delivery systems and its application to HIV treatment; a review. **Int. J. Pharm. Res.,** 2020, 13(1), 659-678. doi:10.31838/ijpr/2021.13.01.085
2. Psimadas D., Georgoulias P., Valotassiou V. and Loudos G.: Molecular nanomedicine towards cancer. **J. Pharm. Sci.,** 2012, 101(7), 2271-2280. doi:10.1002/jps
3. Desai J. and Thakkar H.: Mechanistic evaluation of lymphatic targeting efficiency of atazanavir sulfate loaded lipid nanocarriers: *In vitro* and *in vivo* studies. **J. Drug Deliv. Sci. Technol.,** 2022, 68. doi:10.1016/j.jddst.2021.103090
4. Salah E., Abouelfetouh M. M., Pan Y., Chen D. and Xie S.: Solid lipid nanoparticles for enhanced oral absorption: A review. **Colloids Surf. B,** 2020, 196(7), 111305. doi:10.1016/j.colsurfb.2020.111305
5. Zur Mühlen A., Schwarz C. and Mehnert W.: Solid lipid nanoparticles (SLN) for controlled drug delivery - Drug release and release mechanism. **Eur. J. Pharm. Biopharm.,** 1998, 45(2), 149-155. doi:10.1016/S0939-6411(97)00150-1
6. Uner M. and Yener G.: Importance of solid lipid nanoparticles (SLN) in various administration routes and future perspectives. **Int. J. Nanomed.,** 2007, 2(3), 289-300.
7. Mukherjee S., Ray S. and Thakur R. S.: Solid lipid nanoparticles: A modern formulation approach in drug delivery system. **Indian J. Pharm. Sci.,** 2009, 71(4), 349-358. doi:10.4103/0250-474X.57282
8. Zhang Z., Lu Y., Qi J. and Wu W.: An update on oral drug delivery via intestinal lymphatic transport. **Acta Pharm. Sin. B.,** 2021, 11(8), 2449-2468. doi:https://doi.org/10.1016/j.apsb.2020.12.022
9. Venkateswarlu V.and Manjunath K.: Preparation, characterization and *in vitro* release kinetics of clozapine solid lipid nanoparticles. **J. Control. Release,** 2004, 95(3). 627-638. doi:10.1016/j.jconrel.2004.01.005
10. Patil P., Sharma A., Dadarwal S. and Sharma V.: Development of solid lipid nanoparticles of lamivudine for brain targeting. **Int. J. Drug Deliv. Technol.,** 2009, 1(1). doi:10.25258/ijddt.v1i1.8837
11. Al Haj N. A., Abdullah R., Ibrahim S. and Bustamam A.: Tamoxifen drug loading solid lipid nanoparticles prepared by hot high pressure homogenization techniques. **Am. J. Pharmacol. Toxicol**., 2008, 3(3), 219-224. doi:10.3844/ajptsp.2008.219.224
12. Mirchandani Y. and Patravale V. B.: Solid lipid nanoparticles for hydrophilic drugs, **J. Control. Release,** 2021, 335, 457-464. doi:https://doi.org/10.1016/j.jconrel.2021.05.032
13. Gallarate M., Trotta M., Battaglia L. and Chirio D.: Preparation of solid lipid nanoparticles from W/O/W emulsions: Preliminary studies on insulin encapsulation. **J. Microencapsul.,** 2009, 26(5), 394-402. doi:10.1080/02652040802390156
14. Sansare V., Patel N. and Patankar N.: Design, optimization and characterization of lamivudine loaded solid lipid nanoparticles

for targeted delivery to brain, **Int. Res. J. Pharm.,** 2019, 10(2), 143-148. doi:10.7897/2230-8407.100258

15. Kumar S., Narayan R., Ahammed V., Nayak Y., Naha A. and Nayak U.Y.: Development of ritonavir solid lipid nanoparticles by Box-Behnken design for intestinal lymphatic targeting, **J. Drug Deliv. Sci. Technol.,** 2018, 44, 181-189. doi:https://doi.org/10.1016/j.jddst.2017.12.014
16. Becker P. L., Dearaújo P. H. H. and Sayer C.: Solid lipid nanoparticles for encapsulation of hydrophilic drugs by an organic solvent free double emulsion technique. **Colloids Surf B Biointerfaces,** 2016,140.317-323. doi:10.1016/j.colsurfb.2015.12.033
17. Permana A. D., Tekko I. A. and McCrudden MT. C.: Solid lipid nanoparticle-based dissolving microneedles: A promising intradermal lymph targeting drug delivery system with potential for enhanced treatment of lymphatic filariasis. **J. Control. Release,** 2019, 316, 34-52. doi:10.1016/j.jconrel.2019.10.004
18. Yasir M., Sara UV.S., Chauhan I., Gaur P.K., Singh A.P. and Puri D.: Solid lipid nanoparticles for nose to brain delivery of donepezil: formulation, optimization by Box–Behnken design, *in vitro* and *in vivo* evaluation. **Artif. Cells, Nanomed. Biotechnol.,** 2018, 46(8), 1838-1851. doi:10.1080/21691401.2017.1394872
19. Sharma R. and Mehta K.: Simultaneous spectrophotometric estimation of tenofovir disoproxil fumarate and lamivudine in three component tablet formulation containing efavirenz, **Indian J. Pharm. Sci.,** 2010, 72(4), 527-530. doi:10.4103/0250-474X.73926.
20. Slabiak O. I., Ivanchuk I. M., Klimenko L.Y., Tokaryk G. V. and Kolisnyk I. S.: Development and validation of UV-spectrophotometric procedures for efavirenz quantitative determination, **Int. J. Pharm. Qual. Assur.,** 2018, 9(3), 231-240. doi:10.25258/ijpqa.v9i3.13653
21. Venkatesan S. and Kannappan N.: Simultaneous spectrophotometric method for determination of emtricitabine and tenofovir disoproxil fumarate in Three-Component tablet formulation containing rilpivirine hydrochloride. **Int. Sch. Res. Not.,** 2014, 2014, 1-8. doi:10.1155/2014/541727
22. Kumar C. P., Teja B. R., Varma B. K. and Annapurna M. M.: Derivative and simultaneous equation methods for the determination of fluorometholone and ketorolac in ophthalmic preparations. **Asian J. Pharm.,** 2018, 12(12), S640-S646.
23. Srilatha U., Ramakrishna M., Vasavireddy D. and Devireddy S.R.: Formulation and evaluation of emtricitabine and tenofovir disoproxil fumarate film coated tablets, **IJRPC,** 2015, 116-125.
24. Krishna R. M., Reddy V. D. and Reddy D. S.: Formulation and evaluation of emtricitabine and tenofovir disoproxil fumarate film coated tablets, **IJRPC,** 2015, 2015(1), 116-125. www.ijrpc.com
25. Bazzo G. C., Mostafa D., França M.T., Pezzini B.R. and Stulzer H.K.: How tenofovir disoproxil fumarate can impact on solubility and dissolution rate of efavirenz?, **Int. J. Pharm.,** 2019, 570(7), 118597. doi:10.1016/j.ijpharm.2019.118597
26. Gaur P. K., Mishra S., Bajpai M. and Mishra A.: Enhanced oral bioavailability of efavirenz by solid lipid nanoparticles: *In vitro* drug release and pharmacokinetics studies. **Biomed. Res. Int.,** 2014, 2014. doi:10.1155/2014/363404
27. Sarma A. and Das M. K.: Formulation by Design (FbD) approach to develop tenofovir disoproxil fumarate loaded Nanostructured Lipid Carriers (NLCs) for the aptness of nose to brain delivery, **J. Drug Deliv. Ther.,** 2019, 9(2), 148-159. doi:10.22270/jddt.v9i2.2391
28. Dmitrenko M. E., Penkova A. V. and Atta R.R.: The development and study of novel membrane materials based on polyphenylene isophthalamide - Pluronic®F127 composite, **Mater. Des.,** 2019, 165(January).107596. doi:10.1016/j.matdes.2019.107596
29. Gardouh A.: Design and characterization of glyceryl monostearate solid lipid nanoparticles prepared by High Shear Homogenization. **Br. J. Pharm. Res.,** 2013, 3(3), 326-346. doi:10.9734/bjpr/2014/2770
30. Siram K., Chellan V. R. and Natarajan T.: Solid lipid nanoparticles of diethylcarbamazine citrate for enhanced delivery to the lymphatics: *In vitro* and *in vivo* evaluation, **Expert Opin. Drug Deliv.,** 2014, 11(9), 1351-1365. doi:10.1517/17425247.2014.915310
31. Dinda A., Biswal I., Chowdhury P. and Mohapatra R.: Formulation development and evaluation of paclitaxel loaded solid lipid nanoparticles using glyceryl monostearate, **J. Appl. Pharm. Sci.,** 2013, 3(8), 133-138. doi:10.7324/JAPS.2013.3823
32. Shah R., Eldridge D. and Palombo E.: Harding I. Optimisation and stability assessment of solid lipid nanoparticles using particle size and zeta potential. **J. Phys. Sci.,** 2014, 25(1), 59-75.
33. Paliwal R., Rai S. and Vaidya B.: Effect of lipid core material on characteristics of solid lipid nanoparticles designed for oral lymphatic delivery, **Nanomedicine Nanotechnology, Biol Med.,** 2009, 5(2), 184-191. doi:https://doi.org/10.1016/j.nano.2008.08.003
34. Salvia T. L., Artiga A. M., Molet R. A., Turmo I. A. and Martín B. O.: Emulsion-based nanostructures for the delivery of active ingredients in foods, **Front. Sustain. Food Syst.,** 2018, 2(11), 1-7. doi:10.3389/fsufs.2018.00079